Cement and Concrete Research 39 (2009) 1209–1216

Contents lists available at ScienceDirect

Cement and Concrete Research

journal homepage: http://ees.elsevier.com/CEMCON/default.asp

Prediction of the plastic viscosity of self-compacting steel fibre reinforced concrete

Akbar Ghanbari, Bhushan L. Karihaloo *

School of Engineering, Cardiff University, Cardiff CF24 3AA, UK

ARTICLE INFO

Article history:
Received 18 May 2009
Accepted 25 August 2009

Keywords:
Rheology
Workability
Fresh concrete
Fibre reinforcement
Self-compacting concrete

ABSTRACT

Micromechanical constitutive models are used to predict the plastic viscosity of self-compacting steel fibre reinforced concrete (SCFRC) from the measured plastic viscosity of the paste. The concrete is regarded as a two-phase composite in which the solid phase is suspended in a viscous liquid phase. The liquid matrix phase consists of cement, water and any viscosity modifying agent (VMA) to which the solids (fine and coarse aggregates and fibres) are added in succession. The predictions are shown to correlate very well with available experimental data. Comments are made on the practical usefulness of the predicted plastic viscosity in simulating the flow of SCFRC.

1. Introduction

The rheological study of concrete is of prime importance for the construction industry because concrete is placed in its plastic state. This is even more relevant when dealing with a self-compacting concrete (SCC) [1,2]. However there is as yet no systematic coverage of this topic in the literature. Part of the reason for this may be the various ranges of particle size used in the concrete industry and different devices used to measure the plastic viscosity [3–5] of the heterogeneous concrete mix. The aim of this paper is to develop a micromechanical basis for determining the plastic viscosity of self-compacting concretes with or without short steel fibres from the knowledge of the plastic viscosity of the paste alone. The latter can be measured with a reasonable degree of confidence, whereas the measurement of the plastic viscosity of the concrete mix is fraught with many difficulties and inaccuracies, especially when steel fibres are present. To overcome these, concrete is regarded as a two-phase composite — solid and liquid phases in the present paper. The liquid matrix phase consists of cement, water and any viscosity modifying agent (VMA). The plastic viscosity of this liquid matrix phase is assumed to be known. The increase in plastic viscosity due to the addition of a solid phase (i.e. any cement-replacement materials, fine and coarse aggregates) to this matrix is predicted from the two-phase composite model. The model is applied in stages; in the first stage, the solid phase is the finest solid material which could be the cement-replacement material in the viscous fluid (paste). In the next stage, when the second finest solid (it could be fine aggregate) is added, the composite from the first stage is regarded as the continuous fluid matrix phase. This procedure is continued until all the solid phase constituents have been added to make the SCC.

The plastic viscosity of the viscous concrete consisting of the liquid and solid phases is further increased if steel fibres are added to it. The volume fraction of steel fibres is usually small, so that the dilute approximation is sufficient. In order to estimate the effect of the addition of steel fibres, these are treated by the rigid slender body approximation in a viscous medium [6,7]. The main assumption in this approximation is that the fibres undergo only a rigid body motion in the viscous flow, i.e. translation and rotation, but no elastic deformation. The predictions of this micromechanical approach are shown to correlate very well with available experimental data. Finally, comments are made on the practical usefulness of the predicted plastic viscosity in simulating the flow of SCFRC. It can be used both at the mix design stage to simulate the flow in a cone or an L-box test and at the industrial use stage to simulate the flow in the formwork.

2. Plastic viscosity of self-compacting concrete without steel fibres

2.1. SCC as a concentrated suspension of solid particles in a viscous liquid

The SCC consists of solid aggregate particles (solid phase) suspended in the viscous paste (liquid phase). The particles are modelled as spheres. The viscous behaviour of the resulting suspension depends on the volume fraction of the solid phase. At low concentrations of the solid phase, the plastic viscosity of the suspension does not change much with the shear rate, so that it is reasonable to assume that the suspension behaves like a Newtonian fluid. The behaviour becomes non-Newtonian once the volume fraction of solids reaches a critical value, roughly equal to ϕ_m — the maximum attainable volume concentration which will be defined later. The other parameters influencing the viscosity of the suspension

* Corresponding author.
E-mail address: karihaloob@cardiff.ac.uk (B.L. Karihaloo).

0008-8846/$ – see front matter © 2009 Elsevier Ltd. All rights reserved.
doi:10.1016/j.cemconres.2009.08.018

are the shape, size, and distribution of the solid phase particles, especially at high concentrations.

2.1.1. Low concentration ($\phi < 0.1$)

A low concentration of solid phase is also called dilute, in the sense that the particles are sufficiently far apart from one another, so that the relative motion of the fluid near one particle is unaffected by the presence of the others and the hydrodynamic interaction of the particles can be neglected [8]. Einstein (see, e.g. [9]) was the first to derive the viscosity of a dilute suspension of rigid spheres. He showed that the addition of second phase to a suspension leads to an increase in the bulk viscosity proportional to volume fraction of particles

$$\eta_r = 1 + [\eta]\phi. \tag{1}$$

Here, η_r is the relative viscosity i.e. ratio of viscosity of the suspension (mortar or concrete) to that of the liquid phase (cement paste), ϕ is the volume concentration of particles, and $[\eta]$ is the intrinsic viscosity which is a measure of the effect of individual particles on the viscosity [9]

$$[\eta] = \lim_{\phi \to 0} \frac{\eta_r - 1}{\phi}. \tag{2}$$

A value of $[\eta] = 2.5$ is adopted when the particles are rigid and packed randomly in a hexagonal arrangement, and the distance between them compared to the mean particle diameter is large. It is also important that the movement of the particles is sufficiently slow so that their kinetic energy can be neglected.

Einstein's equation has been widely used by other researchers in this field even at higher volume concentrations of particles. Ford [10] modified Einstein's equation using a binomial expression

$$\eta_r = (1 - [\eta]\phi)^{-1}. \tag{3}$$

As reported by Utracki [11], Simha modified Einstein's relation to read $\eta_r = 1 + 2.5 f(a_1)\phi$, where $f(a_1)$ is the so-called shielding factor, by using a cage model and a reduced volume fraction, ϕ/ϕ_m, where ϕ_m is the maximum packing fraction. In this model each solid spherical particle of radius a is placed inside a spherical enclosure (cage) of radius b. A simplified version of the resulting equation for a low volume concentration can be written as

$$\eta_r = 1 + 2.5\phi\left[1 + \frac{25}{32}\left(\frac{\phi}{\phi_m}\right) - \frac{21}{64}\left(\frac{\phi}{\phi_m}\right)^{\frac{5}{3}} + \frac{625}{128}\left(\frac{\phi}{\phi_m}\right)^2 + \ldots\right]. \tag{4}$$

Based on the Simha calculation for concentrated suspensions, Thomas arrived at the following relation for dilute suspensions [10]:

$$\eta_r = 1 + 2.5\phi\left(1 + \frac{25\phi}{4a_1^3}\right). \tag{5}$$

For low volume fractions, $a_1 = 1.111$.

2.1.2. High concentration ($0.1 < \phi < \phi_m$)

At higher volume concentrations of particles, the volume fraction is not the only parameter that influences the viscosity. It is now necessary to consider the size and type of particles used and their hydrodynamic interaction. The general expression of the viscosity can be written as [10–15]

$$\eta_r = 1 + [\eta]\phi + B\phi^2 + C\phi^3 + \ldots \tag{6}$$

where B (in some references this is called *Huggins coefficient*) and C are very sensitive to the structure of suspension. Tables 1 and 2 give the values of constants B and C that have been reported in the literature [10,15–19].

Table 1
Different values for parameter B available in the literature.

Reference	[10]	[10]	[15]	[16]	[17]	[18]	[19]	[20]
B value	10.05	6.25	4.84	6.2	14.1	7.35	12.6	6

The variation in the cited values of parameters B and C is the result of taking into account one or several effects appearing due to the increase in solid concentration.

Thomas (chapter in [13]) suggested that the C term in Eq. (6) could be replaced by an exponential term

$$\eta_r = 1 + 2.5\phi + 10.05\phi^2 + 0.00273\exp(16.6\phi) \tag{7}$$

because the resulting expression fits the experimental data very well in the range of $\phi = 0.15$–0.60.

In view of the uncertainties in the parameters B and C, Krieger and Dougherty [21], and others, have used the concept of maximum packing fraction, ϕ_m for a better description of the suspensions. ϕ_m corresponds to the situation in which the particles have the minimum possible separation i.e. the void fraction (porosity) is the least and the viscosity is infinite. The value is 0.74 for hexagonal closed packing, 0.637 for random hexagonal packing and 0.524 for cubic packing [10].

Krieger and Dougherty [21] proposed a generalized version of Einstein's equation; they used the maximum packing volume fraction and intrinsic viscosity parameter to a non-Newtonian suspension of rigid spheres. Ball and Richmond [12] used the results of Krieger and Dougherty but simplified their complex mathematics conceptually based on Einstein's equation. In their formulation, the viscosity of the suspension increases in two ways; firstly, if the volume fraction of spherical solid particles increases by $d\phi$, the spheres already present in the suspension raise the total viscosity by $(1/\phi_m)\phi d\phi$, where $1/\phi_m$ is the so-called crowding factor. Therefore, the increment in the viscosity according to Einstein's equation becomes

$$d\eta = [\eta]\eta d\phi + \phi/\phi_m d\eta. \tag{8}$$

Secondly, in the presence of other particles, the volume available for an additional particle is decreased by $(1 - \phi/\phi_m)$ so that the increment in the total viscosity is

$$d\eta = [\eta]\frac{\eta d\phi}{1 - \frac{\phi}{\phi_m}}. \tag{9}$$

Combining the two effects (Eqs. (8) and (9)) they reached the well-known Krieger and Dougherty [21] equation

$$\eta_r = \left(1 - \frac{\phi}{\phi_m}\right)^{-[\eta]\phi_m} \tag{10}$$

ϕ_m is strongly dependent on the particle size distribution. Also, the intrinsic viscosity $[\eta]$ and ϕ_m depend upon the shear rate; the former tends to decrease with increasing shear rate whereas the latter shows the opposite trend. However $[\eta]$ and ϕ_m change in such a way that an increase in the one leads to a decrease in the other, but the product of

Table 2
Different values for parameter C available in the literature.

Reference	[10]	[18]	[20]
C value	15.7	16.2	35

the two changes remains practically the same and equal on average to 1.9 for rigid spheres.

It should be noted that the Krieger and Dougherty equation has been successfully tested by Struble and Sun [9] on cement paste.

Frankel and Acrivos [22] derived theoretically an equation for the viscosity of a very high concentration of solid spheres in suspension, i.e. when $\phi \to \phi_m$

$$\eta_r = \frac{9}{8}\left(\frac{(\phi/\phi_m)^{\frac{1}{3}}}{1-(\phi/\phi_m)^{\frac{1}{3}}}\right). \tag{11}$$

As reported by Shenoy [10], the aim was to derive an expression to complement Einstein's equation for dilute suspension. This equation fits the experimental data for high volume fraction of solid particles rather well.

Chong et al. [23] obtained a single expression to cover the entire range of volume concentrations from $\phi \to 0$ to $\phi \to \phi_m$ which fits the experimental data well

$$\eta_r = \left(1 + \frac{[\eta]\phi_m}{2}\left[\frac{\phi/\phi_m}{1-(\phi/\phi_m)}\right]\right)^2. \tag{12}$$

They added direct Brownian contribution to the viscosity in the range of $\phi/\phi_m \leq 0.7$ because it leads to a slight increase in the relative viscosity. However it should be mentioned that the Brownian contribution can be neglected at higher volume fractions, as confirmed theoretically by Ball and Richmond [12]. Eq. (12) reduces to Einstein's Eq. (1) at low volume fractions.

The drawbacks of applying the ϕ_m-based relations to predict the plastic viscosity of concrete are twofold; firstly, due to the difficulties faced in the measurement of viscosity when ϕ is large ($\phi \to \phi_m$). Secondly, it is difficult to determine the maximum volume fraction accurately because of the swelling in particles, adsorbed surface, etc. (e.g. Ball and Richmond [12]).

2.2. Are the expressions for the viscosity of a suspension of solid particles in a viscous fluid applicable to cement paste?

The theoretical expressions discussed in the previous section are generally applicable to a suspension of solid particles in a viscous fluid at low shear rates. As previously mentioned, the Krieger and Dougherty equation has been used successfully on Portland cement paste and fits the data well. If the concrete in its fresh state is assumed to be an isotropic material then the theory applicable at low shear rates has been demonstrated experimentally by Barnes et al. [12] to be applicable also at high shear rates. They have combined the data from Krieger (reported in [12]) and de Kruif et al. [20] for zero and infinite shear rates and fitted these data to Eq. (10) as shown in Fig. 1.

The effect of shear rate is to alter the packing arrangement. Thus, whilst the packing is random hexagonal at low shear rates, it becomes more and more like closed hexagonal at high rates. The densification of packing at high shear rates is associated with shear thinning such that the product $[\eta]\phi_m$ is constant and equal to about 1.9. It is clear however from Fig. 1 that the shear rate has little influence for volume fractions less than $\phi = 0.4$. However, for comparison with test data which have been obtained at high shear rates, the values of $[\eta]$ and ϕ_m corresponding to the lower curve in Fig. 1 will be used later.

All the above mentioned equations for high volume fraction of particles have been the subject of experimental verification, some of them even on cement-based materials (e.g. Struble and Sun [9]). They give similar predictions in the range of $0.1 < \phi < 0.4$ with only the Frankel and Acrivos [22] equation deviating slightly from the rest (Fig. 2).

Other attempts to derive the viscosity of suspensions based on volume concentration of solid particles can be found in [14].

3. Effect of fibres on the viscosity of SCC

The effect of a dilute concentration (up to 2% by volume) of slender steel fibres on the plastic viscosity of the self-compacting concrete is estimated by applying Russell's slender body approximation, as described by Phan-Thien and Karihaloo [24]. In this approximation, the fibres are treated as slender rigid bodies whose rigid body translation and rotation are restricted as a result of the resistance offered by the viscous self-compacting concrete. Because the fibre is treated as a rigid body, the resisting force may be concentrated at the centroid of the fibre and is equal to [24]

$$F_i = \zeta \dot{u}_i \tag{13}$$

where $\dot{u}_i$ is the component of the displacement rate (i.e. velocity) of the fibre centroid and

$$\zeta = \frac{2\pi\eta l}{\ln(2l_d)} \tag{14}$$

where is η the plastic viscosity of the mix without fibres and l_d is the fibre aspect ratio.

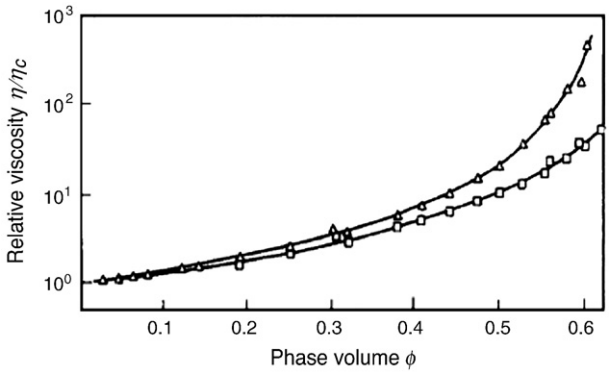

Fig. 1. Dependency of relative viscosity on the shear rate in a suspension at zero and infinite shear rates and fit to the Krieger and Dougherty equation [Fig. 7.8 in Ref. 12].

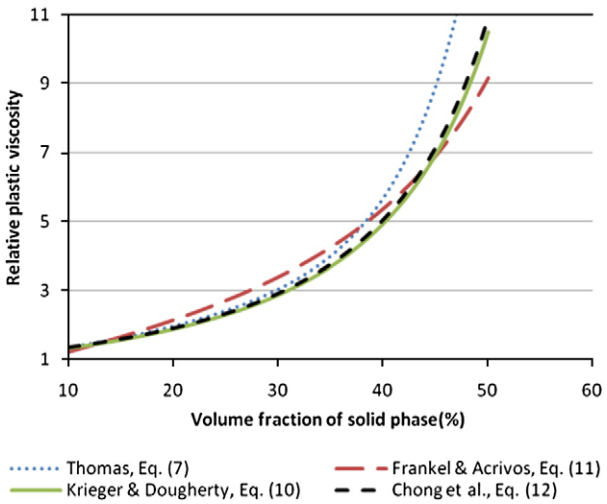

Fig. 2. Comparison of different formulae for high volume fraction of spherical particles with $\Phi_m = 0.708$ and $[\eta] = 2.71$.

Table 3
Estimated plastic viscosity of the paste.

Paste property	Mix1	Mix2	Mix3	Mix4	Mix5	Mix6	Mix7
Paste content (%)	36.5	39.0	36.5	39.0	34.0	36.5	39.0
Paste solid content (%)	53.0	53.7	53.0	53.7	54.5	55.1	55.7
Water/cement	0.42	0.44	0.43	0.44	0.46	0.47	0.47
Plastic viscosity (Pas)	0.44	0.43	0.43	0.43	0.39	0.40	0.41

The superplasticiser to water ratio is 0.02 (0.03 for Mix3) and the superplasticiser to cement ratio is 0.01.

The effective stress tensor of the viscous suspension with matrix designated m and fibres f is

$$\sigma_{ij} = (1-\phi)(\sigma_{ij})_m + (\sigma_{ij})_f \tag{15}$$

where ϕ is the volume fraction of fibres.

The contribution of the fibres can be calculated from

$$(\sigma_{ij})_f = \frac{N}{2}\langle F_i r_j + r_i F_j\rangle \tag{16}$$

where N is the number of fibres, r_i is the component of the position vector of the centroid in the deformed configuration and angular brackets denote ensemble average.

For a statistically homogeneous and random distribution of a dilute concentration of fibres in the viscous matrix such that fibres are unlikely to overlap, the ensemble average can be replaced by volume average over a representative volume element. By definition

$$\phi = Nal = \frac{Nl^3}{l_d^2} \tag{17}$$

where a is the fibre cross-sectional area and l its length.

The effective plastic viscosity of the mix can be obtained by following the procedure of Phan-Thien and Karihaloo [24]. Without going into details it can be shown that the effective shear stress of the viscous suspension is related to the shear rate as follows

$$\sigma_{xy} \equiv \tau = (1-\phi)\eta\dot{\gamma}_{xy} + \frac{\pi\eta\phi l_d^2}{3\ln(2l_d)}\dot{\gamma}_{xy} \tag{18}$$

so that the effective viscosity of the suspension with fibres, $\eta_e = \sigma_{xy}/\dot{\gamma}_{xy}$ is

$$\eta_e = \eta\left\{(1-\phi) + \frac{\pi\phi l_d^2}{3\ln(2l_d)}\right\}. \tag{19}$$

4. Comparison of the proposed formulae with test results

Extensive experimental work has been done on self-compacting fibre reinforced concrete by Grünewald and Walraven [25] who used

Table 4
Mix combinations based on the seven base mixes and the first and second fibre parameters; ϕl_d^2 and $1/\ln(2l_d)$.

Mix designation	No.	Sub-mixes by fibre type, content (kg/m^3) and aspect ratio	ϕl_d^2	$1/\ln(2l_d)$	Measured plastic viscosity (Pas)	Predicted plastic viscosity (Pas)	Error (%)
OS 1-57.0/36.5	1	D-45/30,80,46.3	21.99	0.22	109.90	99.85	10.1
(Mix1)	2	D-45/30,100,46.3	27.48	0.22	137.50	119.39	15.2
	3	D-80/30 BP,40,78.5	31.60	0.20	116.80	126.67	7.8
	4	D-80/30 BP,60,78.5	47.40	0.20	167.80	179.64	6.6
	5	D-80/60 BP,40,85.7	37.66	0.19	122.90	145.53	15.6
OS 2-57.0/39.0	6	D-80/30 BP,60,78.5	47.40	0.20	171.10	149.24	14.6
(Mix2)	7	D-80/30 BP,80,78.5	63.20	0.20	223.20	192.39	16.0
	8	D-80/60 BP,40,85.7	37.66	0.19	98.60	120.83	18.4
	9	D-80/60 BP,60,85.7	56.50	0.19	159.90	172.49	7.3
OS 3-68.0/36.5	10	D-80/30 BP,40,78.5	31.60	0.20	143.10	146.80	2.5
(Mix3)	11	D-80/30 BP,60,78.5	47.40	0.20	199.30	207.85	4.1
	12	D-80/60 BP,40,85.7	37.66	0.19	124.30	154.58	19.6
OS 4-68.0/39.0	13	D-45/30,120,46.3	32.98	0.22	117.50	128.08	8.3
(Mix4)	14	D-45/30,140,46.3	38.48	0.22	145.70	145.27	0.3
	15	D-45/30,160,46.3	43.97	0.22	176.10	162.05	8.7
	16	D-65/40,100,64.9	54.00	0.21	182.40	189.69	3.8
	17	D-65/40,120,64.9	64.80	0.21	221.10	222.05	0.4
	18	D-80/30 BP,60,78.5	47.40	0.20	156.50	166.40	6.0
	19	D-80/30 BP,80,78.5	63.20	0.20	245.30	214.27	14.5
	20	D-80/60 BP,80,85.7	75.33	0.19	199.70	248.43	19.6
OS 5-68.0/34.0	21	D-45/30,100,46.3	27.48	0.22	245.30	206.67	18.7
(Mix5)	22	D-45/30,120,46.3	32.98	0.22	280.30	239.05	17.3
	23	D-80/30 BP,40,78.5	31.60	0.20	195.80	221.20	11.5
	24	D-80/30 BP,60,78.5	47.40	0.20	326.20	312.77	4.3
OS 6-68.0/36.5	25	D-45/30,120,46.3	32.98	0.22	211.50	181.26	16.7
(Mix6)	26	D-80/30 BP,60,78.5	47.40	0.20	266.80	236.21	12.9
	27	D-80/30 BP,80,78.5	63.20	0.20	344.20	303.85	13.3
	28	D-80/60 BP,40,85.7	37.66	0.19	182.80	191.67	4.6
	29	D-80/60 BP,60,85.7	56.50	0.19	301.80	273.01	10.5
OS 7-68.0/39.0	30	D-45/30,120,46.3	32.98	0.22	157.10	147.71	6.4
(Mix7)	31	D-45/30,140,46.3	38.48	0.22	204.40	171.23	19.4
	32	D-65/40,80,64.9	43.20	0.21	155.20	180.56	14.0
	33	D-65/40,100,64.9	54.00	0.21	206.10	218.77	5.8
	34	D-80/30 BP,60,78.5	47.40	0.20	209.10	191.94	8.9
	35	D-80/30 BP,80,78.5	63.20	0.20	306.10	255.68	19.7
	36	D-80/60 BP,60,85.7	56.50	0.19	224.80	221.84	1.3
	37	D-80/60 BP,80,85.7	75.33	0.19	233.10	286.55	18.7

a BML rheometer to measure the viscosity of many mixes. Here only the first seven optimised series (OS) of their mixes have been used and their measured plastic viscosity compared with the predictions. The mix proportions can be found in Ref. [26]. Some of the main parameters were as follows: the size of coarse aggregate varied from 4 to 16 mm, sand from 0.125 to 4 mm, paste volume from 34 to 39%, paste solid content from 53 to 55.7%, water to cement ratio from 0.42 to 0.47. Four types of Dramix steel fibre (RC and RL types) were used with aspect ratios of 46.3, 64.9, 78.5 and 85.7 in concentrations of 80, 100, 120 and 140 kg/m^3 of mix. The fibres replaced the aggregates so that the ratio of sand to total aggregate remained constant.

4.1. Plastic viscosity of cement paste

The plastic viscosity of the paste used in each of the seven SCC mixes [25] is estimated from the data available in the literature that most closely approximates the actual paste used in the mix. It should be mentioned that the plastic viscosity of cement paste is affected by the type and dosage of superplasticiser [27–29], type of cement additives [29,30], mixing sequence and time [31–33], besides the main factors, i.e. the water to cement ratio and amount of superplasticiser in relation to cement and water used. It appears that there is a threshold to the amount of superplasticiser beyond which the plastic viscosity of the paste actually drops.

4.2. Plastic viscosity of SCFRC

Once the plastic viscosity of the paste has been estimated, the increase in plastic viscosity due to the addition of a solid phase (i.e. any cement-replacement materials, fine and coarse aggregates) to this matrix is predicted from the above two-phase composite model. The model is applied in stages; in the first stage, the solid phase is the

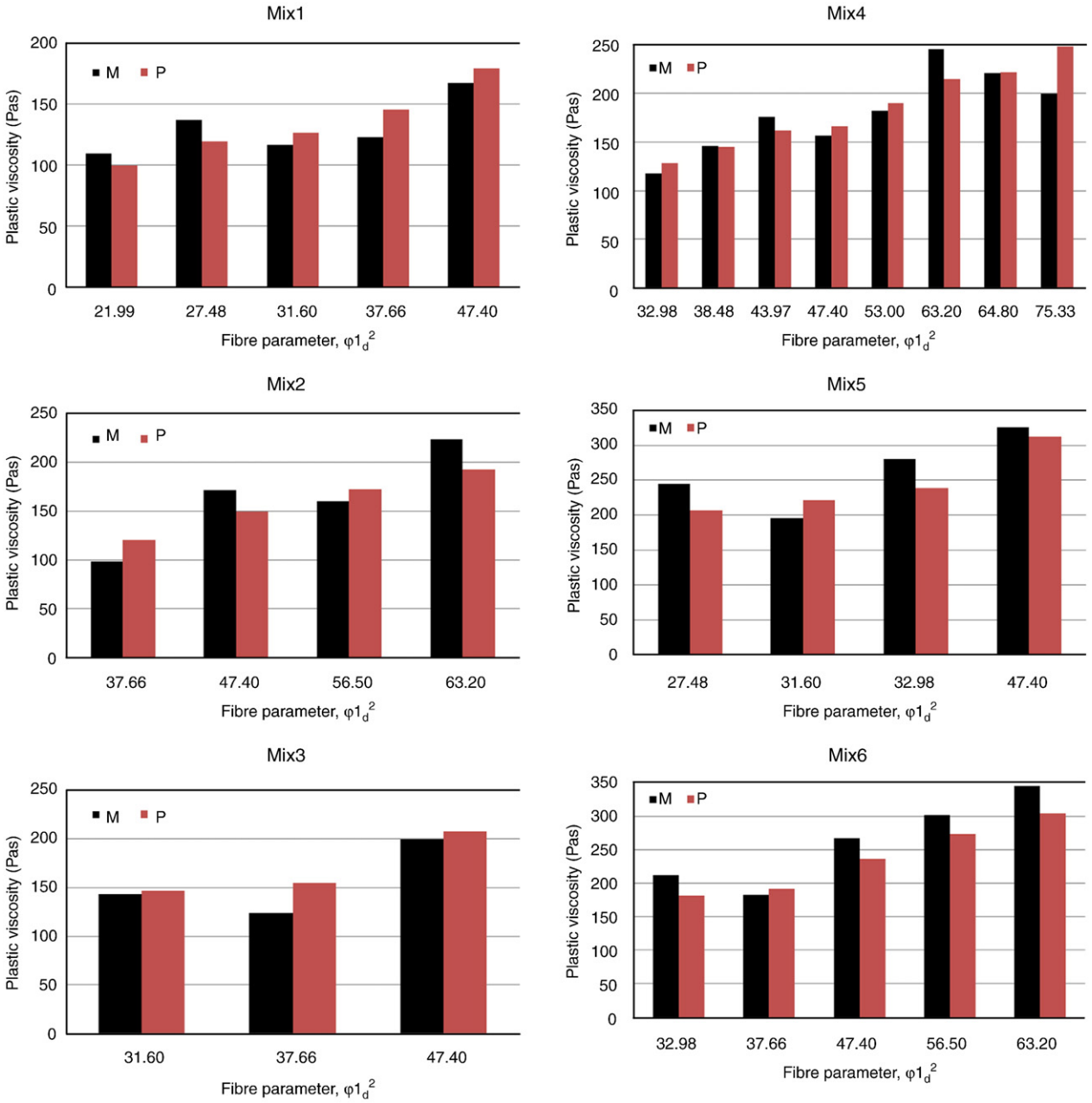

Fig. 3. Comparison of the plastic viscosity with experimental results vs. first fibre parameter, ϕl_d^2 for the seven main mixes with "M" and "P" indicating measured and predicted plastic viscosity.

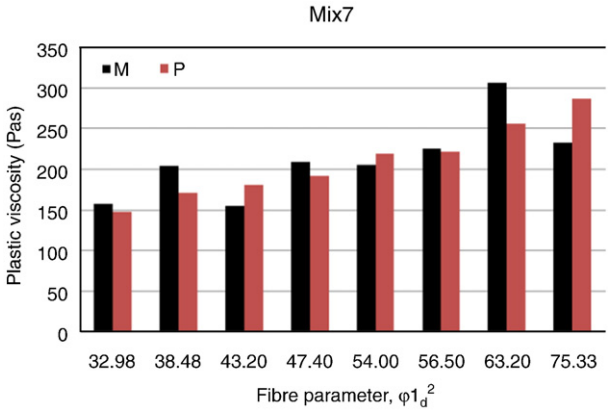

Fig. 3 (*continued*).

finest solid material which could be the cement-replacement material in the viscous fluid (paste). In the next stage when the second finest solid (it could be fine aggregate) is added, the composite from the first stage is regarded as the continuous fluid matrix phase. This procedure is continued until all the solid phase constituents, with the fibres last, have been added to make the SCFRC. The plastic viscosity increase in SCC relative to the fluid phase without fibres is thus

$$\eta_r = f(\phi_1)f(\phi_2)\ldots f(\phi_n) \tag{20}$$

$$\phi_i = \frac{v_i}{v_i + v_0} \tag{21}$$

where

- n total number of solid phases in the mix, such as coarse aggregate, sand, and cement additives;
- v_i volume of solid phase i;
- v_0 volume of the continuous matrix phase in which the solid phase i is suspended;
- $f(\phi_i)$ one of the several two-phase relations introduced in Section 2.1.

Finally to obtain the plastic viscosity of SCC with steel fibres, the result of the application of Eq. (20) to the SCC mix is used in Eq. (19).

Here, the Krieger and Dougherty Eq. (10) will be used as the function $f(\phi)$ in Eq. (20) because it has been found to be most suitable for cement-based mixes [9]. The values correspond to the lower curve in Fig. 2. The plastic viscosity of the paste has been estimated from the data in the literature [27,34–38]; the estimated plastic viscosity of the paste is shown in Table 3, based on the paste content, paste solid content (%) and water to cement ratio.

There are in fact thirty seven different mix combinations formed from the seven basic mixes [26], depending upon the fibre type, fibre content and aspect ratio, as shown in Table 4. We have also introduced two fibre parameters, ϕl_d^2 and $1/\ln(2l_d)$ as they appear in Eq. (19).

4.3. Comparison of the predicted and measured plastic viscosities with respect to first fibre parameter ϕl_d^2

Fig. 3 compares the measured and predicted variations of the plastic viscosity of SCFRC as a function of the first fibre parameter, ϕl_d^2 for all the seven base mixes [25].

4.4. Predicted vs. measured plastic viscosity with respect to second fibre parameter $1/\ln(2l_d)$

It can be seen from Fig. 4 that the predicted plastic viscosity is in very good agreement with the experimental data. The trend line has a high correlation with the second fibre parameter: R^2 factors are 0.96, 0.93, 0.92 and 0.85 for fibre parameter values 0.22, 0.21, 0.20 and 0.19, respectively.

5. Discussion and conclusions

It is clear from Figs. 3 and 4 that the micromechanical relations proposed in this paper are able to predict reasonably accurately the plastic viscosity of SCFRC once the plastic viscosity of the paste is known. The accuracy of the predictions is all the more remarkable given that the plastic viscosity of the paste was not measured but only estimated from similar pastes in the literature. It is quite likely that the predictions would be even more accurate when the viscosity of the paste is measured. The predicted trend, namely that the viscosity increases with increasing fibre parameterϕl_d^2, is consistent with experience which shows that the flow-ability of SCFRC is impaired both when the fibre volume fraction and/or the aspect ratio of the fibre are increased. Some of the measured values however do not follow this expected and correct trend which must therefore be attributed to measurement inaccuracies.

From this study the following conclusions can be drawn. The plastic viscosity of SCFRC can be accurately predicted from the measured viscosity of the paste alone based on micromechanical principles. The latter gives expressions that are accurate for viscous suspensions containing spherical rigid particles in large concentrations and/or needle-shaped rigid steel fibres (with aspect ratio up to 85) in dilute concentrations (up to 2%). For steel fibres in larger concentrations and/or larger aspect ratios, the assumptions that the fibres are rigid and that they are statistically homogeneously distributed in the mix need to be re-examined.

We now comment on the practical usefulness of the proposed model for predicting the plastic viscosity of SCFRC. We note first that the constitutive flow behaviour of SCFRC is best described by the Bingham fluid model (Fig. 5) which requires the plastic yield stress τ_y besides the plastic viscosity. It is however known that, unlike normal

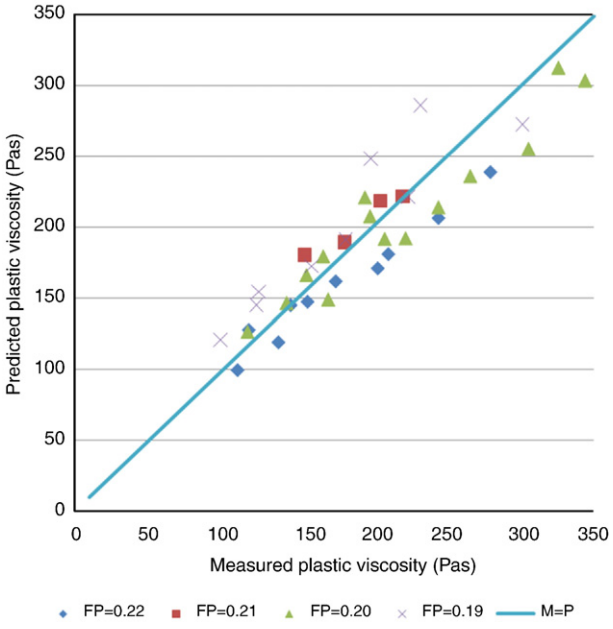

Fig. 4. Predicted vs. experimental plastic viscosity as a function of the second fibre parameter $1/\ln(2l_d)$ for the seven main mixes.

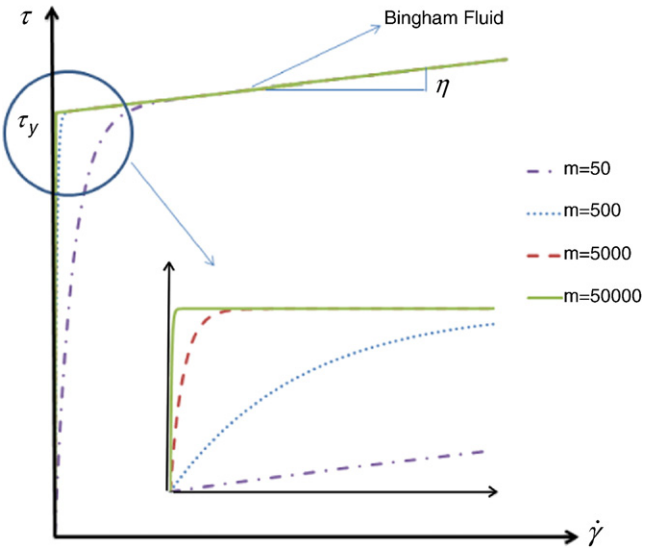

Fig. 5. A bi-linear Bingham fluid constitutive model replaced by the continuous function (22). On the scale of the figure, the discontinuity at τ_y cannot be distinguished for $m=5000$ and 50000. However, at a magnification of 100 on the horizontal scale as shown in the inset, it is clear that the continuous approximation is better for $m=50000$.

concretes and normal fibre reinforced concretes, the yield stress of SCC mixes is nearly constant over a large range of plastic viscosity [39, Fig. 4.3]. Thus, the constitutive relation of a SCFRC mix as a Bingham fluid can be immediately written once its effective plastic viscosity which depends on the mix composition and fibre parameters and the plastic yield stress which depends only on the paste are known. From a practical point of view, it is expedient to represent the bi-linear Bingham model with its associated discontinuity at zero shear rate by a continuous function [40]

$$\tau = \eta\dot{\gamma} + \tau_y(1-e^{-m\dot{\gamma}}) \tag{22}$$

where m is a very large number. It can be seen from Fig. 5 that the continuous function (22) approaches the bi-linear function for large m. The continuous constitutive relation for SCFRC can be used to simulate its flow both at the mix design stage and when it is poured into formwork on site or in a factory. For this simulation, it is of course necessary to use computational tools. Dufour and Pijaudier-Cabot [41] have used the conventional finite element method to simulate the flow of SCC in standard laboratory tests, namely the cone and the L-box tests. We have also used the relation (22) to simulate the flow of an ultra high-performance SCFRC in the cone and L-box tests using the smooth particle hydrodynamic method [42] and compared the results with actual measurements. We have found excellent agreement between the simulated and test results. These simulations will be reported separately elsewhere. We mention finally that the best computational method for simulating the flow of SCFRC using the constitutive relation (22) is the extended finite element method (XFEM) [43] because it avoids the need for re-meshing at the moving boundary between the SCFRC and air as it is poured into the formwork. We are currently exploring this simulation method.

References

[1] G. Heirman, L. Vandewalle, D. Van Gemert, Ó. Wallevik, Integration approach of the Couette inverse problem of powder type self-compacting concrete in a wide-gap concentric cylinder rheometer, Journal of Non-Newtonian Fluid Mechanics 150 (2008) 93–103.
[2] J.-Y. Petit, E. Wirquin, Y. Vanhove, K. Khayat, Yield stress and viscosity equations for mortars and self-consolidating concrete, Cement and Concrete Research 37 (2007) 655–670.
[3] A.I. Laskar, S. Talukdar, Rheological behavior of high performance concrete with mineral admixtures and their blending, Construction and Building Materials 22 (2008) 2345–2354.
[4] K.G. Kuder, N. Ozyurt, E.B. Mu, S.P. Shah, Rheology of fiber-reinforced cementitious materials, Cement and Concrete Research 37 (2007) 191–199.
[5] M. Westerholm, B. Lagerblad, J. Silfwerbrand, E. Forssberg, Influence of fine aggregate characteristics on the rheological properties of mortars, Cement and Concrete Composites 30 (2008) 274–282.
[6] W.B. Russel, On the effective moduli of composite materials: effect of fiber length and geometry at dilute concentrations, Zeitschrift für Angewandte Mathematik und Physik (ZAMP) 24 (1973) 581–600.
[7] N. Phan-Thien, R.R. Huilgol, A micromechanic theory of chopped-fibre-reinforced materials, Journal of Fibre Science and Technology 13 (1980) 423–433.
[8] G.K. Batchelor, The stress generated in a non-dilute suspension of elongated particles by pure straining motion, Journal of Fluid Mechanics Digital Archive 46 (1971) 813–829.
[9] L. Struble, G.-K. Sun, Viscosity of Portland cement paste as a function of concentration, Advanced Cement Based Materials 2 (1995) 62–69.
[10] A.V. Shenoy, Rheology of Filled Polymer Systems, Springer, 1999, pp. 136–149.
[11] L.A. Utracki, Polymer Blends Handbook, Springer, 2003, pp. 459–461.
[12] H.A. Barnes, J.F. Hutton, K. Walters, An Introduction to Rheology, Elsevier, 1993, pp. 119–128.
[13] K.L. Mittal, P. Kumar, Handbook of Microemulsion Science and Technology, CRC Press, 1999, pp. 357–362.
[14] R.K. Gupta, Polymer and Composite Rheology, CRC Press, 2000, pp. 177–179.
[15] J.R. Willis, J.R. Acton, Quarterly Journal of Mechanics and Applied Mathematics 29 (1976) 163–177.
[16] G.K. Batchelor, The effect of Brownian motion on the bulk stress in a suspension of spherical particles, Journal of Fluid Mechanics Digital Archive 83 (1977) 97–117.
[17] E. Guth, A.R. Simha, Viscosity of suspensions and solutions, Kolloid-Z 74 (1936) 266.
[18] V. Vand, Viscosity of solutions and suspensions. II, Experimental determination of the viscosity & concentration function of spherical suspensions, The Journal of Physical and Colloid Chemistry 52 (1948) 300–314.
[19] N. Saito, Concentration dependence of the viscosity of high polymer solutions. I, Journal of the Physical Society of Japan 5 (1950) 4–8.
[20] C.G. de Kruif, E.M.F. van Iersel, A. Vrij, W.B. Russel, Hard sphere colloidal dispersions: viscosity as a function of shear rate and volume fraction, The Journal of Chemical Physics, AIP (1985) 4717–4725.
[21] I.M. Krieger, T.J. Dougherty, A mechanism for non-Newtonian flow in suspensions of rigid spheres, Journal of Rheology 3 (1959) 137–152.
[22] N.A. Frankel, A. Acrivos, On the viscosity of a concentrated suspension of solid spheres, Chemistry and Engineering Science 22 (1967) 847–853.
[23] J.S. Chong, E.B. Christiansen, A.D. Baer, Rheology of concentrated suspensions, Journal of Applied Polymer Science 15 (1971) 2007–2021.
[24] N. Phan-Thien, B.L. Karihaloo, Materials with negative poisson's ratio: a qualitative microstructural model, Journal of Applied Mechanics 61 (1994) 1001–1004.
[25] S. Grünewald, J.C. Walraven, Rheological measurements on self-compacting fibre reinforced concrete, in: Ó. Wallevik, I. Níelsson (Eds.), Proceedings of the 3rd International RILEM Symposium on Self-Compacting Concrete, RILEM S.A.R.L, France, 2003, pp. 49–58.
[26] S. Grünewald, Performance-based design of self-compacting fibre reinforced concrete, Ph.D. Thesis of Delft university (Netherlands), 2004 pp. 48–61.
[27] M. Lachemi, K.M.A. Hossain, V. Lambros, P.C. Nkinamubanzi, N. Bouzoubaâ, Performance of new viscosity modifying admixtures in enhancing the rheological properties of cement paste, Cement and Concrete Research 34 (2004) 185–193.
[28] N. Mikanovic, C. Jolicoeur, Influence of superplasticizers on the rheology and stability of limestone and cement pastes, Cement and Concrete Research 38 (2008) 907–919.
[29] M. Cyr, C. Legrand, M. Mouret, Study of the shear thickening effect of superplasticizers on the rheological behaviour of cement pastes containing or not mineral additives, Cement and Concrete Research 30 (2000) 1477–1483.
[30] C.F. Ferraris, K.H. Obla, R. Hill, The influence of mineral admixtures on the rheology of cement paste and concrete, Cement and Concrete Research 31 (2001) 245–255.
[31] I. Aiad, S. Abd El-Aleem, H. El-Didamony, Effect of delaying addition of some concrete admixtures on the rheological properties of cement pastes, Cement and Concrete Research 32 (2002) 1839–1843.
[32] V. Fernàndez-Altable, I. Casanova, Influence of mixing sequence and super-plasticiser dosage on the rheological response of cement pastes at different temperatures, Cement and Concrete Research 36 (2006) 1222–1230.
[33] D.A. Williams, A.W. Saak, H.M. Jennings, The influence of mixing on the rheology of fresh cement paste, Cement and Concrete Research 29 (1999) 1491–1496.
[34] P. Chindaprasirt, S. Hatanaka, T. Chareerat, N. Mishima, Y. Yuasa, Cement paste characteristics and porous concrete properties, Construction and Building Materials 22 (2008) 894–901.
[35] Z. Sun, T. Voigt, S.P. Shah, Rheometric and ultrasonic investigations of viscoelastic properties of fresh Portland cement pastes, Cement and Concrete Research 36 (2006) 278–287.
[36] S. Grzeszczyk, G. Lipowski, Effect of content and particle size distribution of high-calcium fly ash on the rheological properties of cement pastes, Cement and Concrete Research 27 (1997) 907–916.
[37] M. Nehdi, M.A. Rahman, Estimating rheological properties of cement pastes using various rheological models for different test geometry, gap and surface friction, Cement and Concrete Research 34 (2004) 1993–2007.
[38] X. Zhang, J. Han, The effect of ultra-fine admixture on the rheological property of cement paste, Cement and Concrete Research 30 (2000) 827–830.

[39] J. Dransfield, Admixtures for concrete, mortar and grout, in: J. Newman, B.S. Choo (Eds.), Advanced Concrete Technology, vol. 2, Elsevier, 2003, (Ch 4).
[40] T.C. Papanastasiou, Flows of materials with yield, Journal of Rheology 31 (1987) 385–404.
[41] F. Dufour, G. Pijaudier-Cabot, Numerical modelling of concrete flow: homogeneous approach, International Journal for Numerical and Analytical Methods in Geomechanics 29 (2005) 395–416.
[42] J. Bonet, S. Kulasegaram, Correction and stabilization of smooth particle hydrodynamic methods with application in metal forming simulations, International Journal of Numerical Methods in Engineering 47 (2000) 1189–1214.
[43] Q.Z. Xiao, B.L. Karihaloo, Modelling of stationary and growing cracks in FE framework without remeshing: a state-of-the-art review, Computers and Structures 81 (2003) 119–129.